

# Discovery and Pharmacological Characterization of JNJ-42756493 (Erdafitinib), a Functionally Selective Small-Molecule FGFR Family Inhibitor



Timothy P.S. Perera<sup>1</sup>, Eleonora Jovcheva<sup>1</sup>, Laurence Mevellec<sup>2</sup>, Jorge Vialard<sup>1</sup>, Desiree De Lange<sup>1</sup>, Tinne Verhulst<sup>1</sup>, Caroline Paulussen<sup>1</sup>, Kelly Van De Ven<sup>1</sup>, Peter King<sup>1</sup>, Eddy Freyne<sup>1</sup>, David C. Rees<sup>3</sup>, Matthew Squires<sup>3</sup>, Gordon Saxty<sup>3</sup>, Martin Page<sup>1</sup>, Christopher W. Murray<sup>3</sup>, Ron Gilissen<sup>1</sup>, George Ward<sup>3</sup>, Neil T. Thompson<sup>3</sup>, David R. Newell<sup>4</sup>, Na Cheng<sup>5</sup>, Liang Xie<sup>5</sup>, Jennifer Yang<sup>5</sup>, Suso J. Platero<sup>6</sup>, Jayaprakash D. Karkera<sup>6</sup>, Christopher Moy<sup>6</sup>, Patrick Angibaud<sup>2</sup>, Sylvie Laquerre<sup>6</sup>, and Matthew V. Lorenzi<sup>6</sup>

## Abstract

Fibroblast growth factor (FGF) signaling plays critical roles in key biological processes ranging from embryogenesis to wound healing and has strong links to several hallmarks of cancer. Genetic alterations in FGF receptor (FGFR) family members are associated with increased tumor growth, metastasis, angiogenesis, and decreased survival. JNJ-42756493, erdafitinib, is an orally active small molecule with potent tyrosine kinase inhibitory activity against all four FGFR family members and selectivity versus other highly related kinases. JNJ-42756493 shows rapid uptake into the lysosomal compartment of cells in culture, which

is associated with prolonged inhibition of FGFR signaling, possibly due to sustained release of the inhibitor. In xenografts from human tumor cell lines or patient-derived tumor tissue with activating FGFR alterations, JNJ-42756493 administration results in potent and dose-dependent antitumor activity accompanied by pharmacodynamic modulation of phospho-FGFR and phospho-ERK in tumors. The results of the current study provide a strong rationale for the clinical investigation of JNJ-42756493 in patients with tumors harboring FGFR pathway alterations. *Mol Cancer Ther*; 16(6); 1010–20. ©2017 AACR.

## Introduction

Fibroblast growth factor receptors belong to a family of 4 receptor tyrosine kinases (FGFR1–4) and a fourth receptor (FGFR5) lacking a tyrosine kinase domain (1, 2). FGFRs have been demonstrated to regulate a number of key processes, such as cell migration, proliferation, differentiation, and survival, particularly during embryonic development and in the adult organism during inflammation and wound healing (1, 2). FGFR activity is controlled by a family of FGF ligands, comprised of 22 FGF members (3) that regulate FGFR tyrosine kinase activity in an autocrine or paracrine tissue-dependent context (4). A key example of FGFR ligand-regulated physiology is the regulation of

phosphate homeostasis mediated by FGF23, which suppresses phosphate reabsorption in proximal tubules of the kidney (5). In contrast, constitutive ligand-independent and aberrant ligand-dependent FGFR signaling have been described in a large variety of solid tumors, including non-small cell lung, breast, bladder, endometrial, gastric, and colon cancer, as well as certain hematological malignancies. Aberrant pathway activation is believed to be a key growth promoting mechanism for these malignancies (1–16). Further support of this concept is highlighted by the presence of activating FGFR gene alterations, including point mutations and gene rearrangements, in multiple tumor types, suggesting that deregulated proliferation of certain tumors is driven by these oncogenic events (7, 17). Given the activation of FGFR signaling in a variety of tumor types, several therapeutic agents, including multiple FGFR inhibitors, FGFR antibodies, and FGF ligand traps, have been optimized and tested clinically or are entering into clinical development (18). Most of these small molecule inhibitors have limited selectivity for FGFR and display significant activity against additional protein tyrosine kinases due to high sequence homology within their kinase domains [e.g., vascular endothelial growth factor (VEGFR), platelet-derived growth factor (PDGFR) and c-Kit]. The activities of these mixed FGFR/VEGFR inhibitors make it difficult to dissect the antitumor activity components associated with FGFR inhibition versus other inhibitory events leading to potential additional toxicities compared with selective inhibitors.

To better address the role of constitutive FGFR signaling in cancer, we optimized a next-generation small-molecule

<sup>1</sup>Janssen Research and Development, Beerse, Belgium. <sup>2</sup>Janssen Research and Development, Val de Reuil, France. <sup>3</sup>Astex Pharmaceuticals, Cambridge, United Kingdom. <sup>4</sup>Newcastle Cancer Centre, Northern Institute for Cancer Research, Newcastle University, Newcastle upon Tyne, United Kingdom. <sup>5</sup>Janssen Research and Development, Shanghai, China. <sup>6</sup>Janssen Research and Development, Spring House, Pennsylvania.

**Note:** Supplementary data for this article are available at Molecular Cancer Therapeutics Online (<http://mct.aacrjournals.org/>).

**Corresponding Author:** Matthew V. Lorenzi, Oncology Discovery, Janssen Research and Development, 1400 McKean Street, Spring House, PA 19477. Phone: 215-793-7356; Fax: 215-540-4763; E-mail: [mlorenzi@its.jnj.com](mailto:mlorenzi@its.jnj.com)

**doi:** 10.1158/1535-7163.MCT-16-0589

©2017 American Association for Cancer Research.

inhibitor that is highly selective for the FGFR kinase family with minimal inhibitory activity toward VEGFR and other related kinases. Here, we report the identification and pharmacologic characterization of JNJ-42756493 (erdafitinib) as a novel, highly potent and selective, small-molecule inhibitor of FGFR1-4. This study demonstrates functional selectivity of erdafitinib in tumor models with constitutive FGFR activity and supports the ongoing clinical development of this agent in disorders associated with FGFR activation.

## Materials and Methods

### JNJ-42756493

JNJ-42756493 (Fig. 1A), N-(3,5-Dimethoxy-phenyl)-N'-isopropyl-N-[3-(1-methyl-1 H-pyrazol-4-yl)-quinoxalin-6-yl]-ethane-1,2-diamine, was synthesized according to the processes described in the International Patent Application Number WO2011/135376 in particular as described, for example, B3 (compound 4). JNJ-42756493 (446.56MW of free base) has no chiral center, is basic (pKa of 9.2), and lipophilic (logP = 4.3). It is a crystalline, auto-fluorescent (Exc 370 nm; Emm 490 nm), non-hygroscopic solid, with a melting point of 142°C and a high thermodynamic solubility of >20 mg/mL in aqueous buffer at pH = 4. JNJ-42756493 in 5 mmol/L dimethyl sulphoxide (DMSO) stock was used for *in vitro* or was formulated for *in vivo* studies in 20% hydroxypropyl- $\beta$ -cyclodextrin (HP- $\beta$ -CD) for oral gavage either once or twice daily.

### Time-resolved fluorescence kinase assays for FGFR1-4 and KDR

Time-resolved fluorescence energy-transfer assays for FGFR1-4 and KDR were performed in 384-well black Optiplates (Perkin Elmer, 6007279). Enzymes [FGFR1 (Upstate, 14-582-4)].

FGFR2 (Invitrogen, PV4106), FGFR3 (Upstate, 14-464-K), FGFR4 (Upstate, 14-593-K), and KDR (Upstate, 14-630-K), substrate (FLT 3 peptide, Bachem, 4072151), and adenosine triphosphate (ATP, Invitrogen, PV3227) were prepared in 50 mmol/L HEPES pH 7.5, 0.1 mmol/L Na<sub>2</sub>VO<sub>3</sub>, 6 MnCl<sub>2</sub>, 0.01% (v/v) Triton x-100, and 1 mmol/L dithiothreitol (DTT). Detection reagents were prepared in 6.25 mmol/L HEPES, 0.025% BSA, 7 mmol/L EDTA, 31.25 nmol/L streptavidin-XL665 (CIS-BIO, 610SAXLB), and 2.27 nmol/L Eu-labeled PY20 antibody (Perkin Elmer, AD0067). The kinase reaction was initiated by addition of enzyme (0.1, 0.8, 0.8, 0.4, and 0.7 nmol/L of FGFR 1, 2, 3, 4, and KDR, respectively) to a mixture containing compound, ATP at the Michaelis constant (Km) concentration for each kinase (5, 0.4, 25, 5, and 3  $\mu$ mol/L, respectively) and 500 nmol/L FLT3 substrate in a final assay volume of 30  $\mu$ L. After 60 minutes for FGFR1, FGFR3, and KDR, 30 minutes for FGFR2 and 45 minutes for FGFR4 incubation at room temperature, the enzyme reaction was stopped by adding 10  $\mu$ L of detection reagents. Following 1-hour incubation at room temperature, fluorescence was measured with excitation at 337 nm and dual emission at 620 nm (Eu signal) and 665 nm (FRET signal) on an Envision reader (Perkin Elmer, 2104-0010A).

### Kinase binding assays

The binding affinity of JNJ-42756493 to a panel of 397 wild-type kinases was evaluated using the KINOMEScan platform (DiscoverX; ref. 19).

### Cellular kinase assays

IL3-dependent (10 ng/mL final concentration) murine BaF3 (Riken Cell Bank) pro-B cells (20) were transfected with pcDNA3.1 (Invitrogen) plasmid encoding TEL(ETV6)-kinase and stable integrations selected with geneticin (Invitrogen; ref. 21). GFP-TEL-FGFR1 and GFP-TEL-KDR(VEGFR2) were kindly provided by Jan Cools (Department of Human Genetics, University of Leuven).

### Cell lines

The tumor cell lines used for Western blotting and the small panel tested in proliferation experiments were obtained from the American Type Culture Collection (ATCC), unless specified otherwise. KATO III (HTB-103), SNU-16 (CRL-5974), RT-112 (DSMZ ACC 418), NCI-H1581 (CRL-5878), A-204 (HTB-82), RT-4 (HTB-2), DMS-114 (CRL-2066), A-427 (HTB-53), KMS-11 (Japanese Collection of Research Bioresources), and MDA-MB-453 (HTB-131) cells were selected to reflect diverse FGFR alterations. All cell lines were obtained between 2012 and 2016 and kept in culture up to 15 to 20 passages, but not longer than 6 months. All cell lines were authenticated by the suppliers using short tandem repeat (STR) analysis. Cells were cultured as suggested by the supplier in standard culture conditions (37°C, 5% CO<sub>2</sub>, and 95% humidity) in medium containing 10% (v/v) fetal bovine serum. Kato III cells were supplemented with 2 mmol/L L-glutamine, 1.5 g/L sodium bicarbonate, 50  $\mu$ g/mL gentamycin, and 20% FBS. Cells were free of mycoplasma.

The cell lines tested in the extended panel of the growth assay were obtained from the ATCC (22), the German Collection of Microorganisms and Cell Cultures (23), and the Japanese Collection of Research Bioresources (24) and cultured as described above.

Cell lines were annotated for somatic alterations using the data compiled by OmicSoft ArraySuite software, version 8. Original source data are derived from the Cell Line Encyclopedia (<https://www.broadinstitute.org/ccle/home>) and Sanger Center Cancer Cell Line Project, available on the COSMIC website (<http://cancer.sanger.ac.uk/cosmic>).

### MTT assay for cell proliferation

KATO III, RT-112, A-204, RT-4, DMS-114, A-427, and MDA-MB-453 cells were treated with JNJ-42756493 (from 10  $\mu$ mol/L to 0.01 nmol/L in 2% DMSO, final concentration). Following 4-day incubation, cell viability was determined using MTT reagent as described by the supplier (Sigma, CGD1). The optical density was determined at 540 nm as a percentage of DMSO-treated cells (100%), a dose-response curve was created and the median inhibition concentration (IC<sub>50</sub>) calculated.

### Alamar Blue assay for cell proliferation

SNU-16, NCI-H1581, KMS-11, and BaF3 cells were treated with compound for 4 days as described above. Alamar Blue solution was added as described by the manufacturer (Sigma, R7017) and incubated for an additional 4 hours. Fluorescence was measured (excitation wavelength 530–560 nm, emission wavelength 590 nm) and expressed as a percentage of untreated control. From these data, a dose-response curve was created and IC<sub>50</sub> values determined.

### Large panel all cancer and lung cancer cell lines

Cancer cells were grown as specified by the provider (Oncolead, GmbH & Co. KG). At 24 hours post seeding, cells were treated in triplicate with small-molecule FGFR inhibitor serially diluted 3.16-fold over 10 concentrations (0.5% DMSO final concentration). Following 72-hour incubation, cells were fixed and stained with a nuclear dye for quantification of proliferation. To determine the cell proliferation endpoint, data were transformed to percent of control (POC) values [ $100 \times$  relative cell count (drug treatment)/relative cell count (vehicle treatment)]. IC<sub>50</sub> values were estimated from a nonlinear regression fit of the POC data to a 1-site dose-response model.

### Inhibition of FGFR family receptor phosphorylation and downstream signaling

Cell lines harboring activated FGFR1, 2, 3, or 4 (NCI-H1581, SNU-16, KMS-11, and MDA-MB453, respectively) were treated with various concentrations of JNJ-42756493 for 4 hours. Medium was removed, cells washed with ice-cold phosphate buffered saline (PBS) and suspended in lysis buffer for Western blotting analysis.

The NCI-H1581 NSCLC cell line was pretreated with medium containing 100 nmol/L JNJ-42756493 or DMSO for 30 minutes prior to replacement with medium containing FGF2 (40 ng/mL). The cells treated with FGF2 were incubated for 0 minute (control, no treatment with FGF2), 5 minutes, 10 minutes, 30 minutes, 2 hours, 4 hours, or 8 hours. The medium was aspirated, the cells were washed with ice-cold PBS, lysed, and processed for Western blot analysis.

### Western blotting

Cell lysates were loaded on NuPAGE Novex Bis-Tris Mini Gels and transferred to poly vinylidene-difluoride (PVDF) membranes. Primary antibodies were incubated as specified, membrane washed 3 times in PBS-0.1% Tween-20, and fluorescently labeled secondary antibody incubated for 1 hour at room temperature in the dark. Membranes were washed 3 times and antibody binding detected using Lumi Proxima or LI-COR Odyssey instruments. Antibodies against ERK, pERK (Thr202/Tyr204), pFGFR (Tyr653/654), and pPLCg1 (Tyr783) were obtained from Cell Signaling Technology (#9101, #9102, #3471, and #2821, respectively), FGFR2 and FRS2 $\alpha$  from Santa Cruz Biotechnology (SC #3471, SC #8318, respectively), and  $\beta$ -actin from Calbiochem (# CP01). Secondary antibodies were obtained from Invitrogen [goat anti-rabbit IgG HRP (A21076), goat anti-mouse IgG HRP (A21057), goat anti-mouse (A21057), and goat anti-rabbit (A21076)].

### Lysosomal compound accumulation

GAMG human glioblastoma cells (DSMZ, ACC 242) were treated for 30 minutes with 50 nmol/L LysoTracker red and 1  $\mu$ mol/L JNJ-42756493 before imaging at 530 nm. GAMG cells were treated with bafilomycin (75 nmol/L) for 1 hour and washed with PBS before addition of medium supplemented with 1  $\mu$ mol/L JNJ-42756493 or JNJ-42883919 in the presence or absence of 75 nmol/L bafilomycin. Serial images were obtained every 5 minutes (ImageJ) in Texas Red and CFP channels on an InCell Analyzer 2000 instrument. The density of region of interest (ROI) from 4 different images was compared with T = 0 and the average difference plotted as percentage change (%ROI).

### Drug washout assays

KATO III human gastric carcinoma cells were treated with or without bafilomycin (150 nmol/L) for 1 hour before addition of JNJ-42756493 (30 nmol/L) or JNJ-42883919 (300 nmol/L) to the culture medium. The medium was removed, cells were washed 6 times with warm medium with or without bafilomycin, and then incubated in medium lacking compounds and bafilomycin. Cells were collected at 0, 2, 4, 8, 16, and 24 hours, lysates prepared and processed for WES capillary-based Western blotting as described by the manufacturer (ProteinSimple).

### In vivo efficacy experiments

All experiments were carried out in accordance with the European Communities Council Directives (86/609/EEC) and approved by the local IACUC and ethical committee. For tumor efficacy studies, tumor sizes [tumor volume (mm<sup>3</sup>) = ( $a \times b^2/2$ ); where  $a$  represents the length, and  $b$  the width of the tumor as determined by caliper measurements] and body weights were measured twice weekly, with mice monitored daily for clinical signs of toxicity [including but not limited to persistent anorexia, dehydration, posture, lethargy (according to the United Kingdom Coordinating Committee for Cancer Research (UKCCCR) guidelines for welfare of animals in experimental neoplasia ref. 25] for the duration of the treatment. A sustained body weight loss >15% of the initial body weight was considered as clinical toxicity, with the animal removed from the study and sacrificed. Studies were terminated when tumor burden exceeded 10% of the animal's body weight. Time-course of tumor growth was expressed as relative tumor volumes, normalized to initial tumor volume (day treatment started) and expressed as mean  $\pm$  standard error of mean (SEM). Treatment/control (T/C) ratios were calculated based on the change in final relative tumor volumes, and National Cancer Institute's (NCI) effective criteria of 42% were used (26).

Human tumor cell lines were injected directly into the inguinal region of male nude mice ( $1 \times 10^7$  cells/200  $\mu$ L/animal with Matrigel 1:1 in medium) on day 0. When tumors were established, mice were randomized according to tumor volume to either vehicle alone (10% HP- $\beta$ -CD) or vehicle containing JNJ-42756493, administered in a volume of 5 mL/kg body weight for 21 days (8–10 mice/group). For PDX studies, Nu/Nu nude mice purchased from Vital River Lab Animal Technology Co., Ltd.. Patient-derived tumor samples finely minced ( $\sim 1$ –2 mm<sup>3</sup>) were added to Matrigel and approximately 50 mm<sup>3</sup> of minced tumor was implanted subcutaneously (s.c.) into flank of anaesthetized mice (Ketamine/Medetomidine). When the tumor volume reached 200 to 300 mm<sup>3</sup> the mice were allocated to their treatment groups with uniform mean tumor volume and body weight between groups and treated according to protocol.

### Pharmacodynamic and pharmacokinetic analysis of JNJ-42756493

Mice-bearing SNU-16 human gastric carcinoma (FGFR2 amplified) xenograft tumors were dosed orally with 0, 3, 10, or 30 mg/kg JNJ-42756493. Tumor tissue and mouse plasma (3 mice per time point) were harvested at 0.5, 1, 3, 7, 16, and 24 hours after dosing. Tumor tissues were frozen in liquid nitrogen, crushed, and suspended in lysis buffer [25 mmol/L Tris-HCl (pH 7.5), 2 mmol/L EDTA (pH 8), 2 mmol/L EGTA (pH8), 1% Triton X-100, 0.1% SDS, 50 mmol/L disodium  $\beta$ -glycerophosphate, 2 mmol/L Na<sub>3</sub>VO<sub>4</sub>, 4 mmol/L Na-pyrophosphate,

2x Thermo protease/phosphatase inhibitor cocktail). After centrifugation (12,000 rpm for 15 minutes; RCF = 15,294), the supernatants were applied to SDS-PAGE and transferred onto PVDF membranes (Bio-Rad, #162-0177). The membranes were blocked in Odyssey blocking buffer (Licor, #927-40000) for 1 hour, incubated with anti-phospho-FGFR Y653/654 (Cell Signaling Technology, #3471) or anti-FGFR2 (Cell Signaling Technology, #9102) antibodies overnight at 4°C, and washed 3 times in TBST buffer prior to incubation with Alexa Fluor 680 conjugated goat-anti-rabbit IgG (#A-21109) in Odyssey blocking buffer at room temperature for 2 hours. Signals were read and quantitated on a LI-COR Odyssey infrared imager.

When tumors of lung cancer patient-derived xenograft (PDX, LUX001) reached approximately 400 mm<sup>3</sup>, mice were dosed orally with 12.5 mg/kg JNJ-42756493. Tumor and mouse plasma (3 mice per time point) were collected at 1, 2, 4, 8, and 24 hours post dose. The liquid nitrogen frozen tumor tissues were lysed in RIPA buffer containing protease inhibitor (Roche, Cat#04693132001) and phosphatase inhibitor (Roche, Cat#04906837001). After centrifugation (12,000 rpm for 15 minutes), the supernatants were applied to SDS-PAGE and transferred onto PVDF membranes (Bio-Rad #170-4157). The membrane was blocked in 5% bovine serum albumin in

Tris-buffered saline with 0.1% Tween 20 (TBST) and then incubated with anti-phospho-ERK (Cell Signaling Technology, #4370) overnight at 4°C, washed in TBST, then incubated with HRP-conjugated goat Anti-Rabbit IgG (H+L; Bio-Rad, 1706515) at room temperature for 2 hours. The membranes were stripped and reblotted for total ERK1/2 (Cell Signaling Technology, #9102). Signal was read on ChemiDoc™ MP Imaging System.

Compound concentration from mouse plasma was detected using LC/MS-MS.

## Results

### JNJ-42756493 is a potent and selective pan-FGFR inhibitor

The hinge binding motif, quinoxaline scaffold of JNJ-42756493 (Table 1), was identified following a fragment-based screen of the Astex proprietary library (20). Quinoxaline containing fragments were further modified by introducing the 3,5-dimethoxy aniline moiety beyond the gatekeeper in the selectivity pocket. Taking advantage of aniline nitrogen positioning, substituents interacting with Asp641 were introduced that ultimately led to selection of JNJ-42756493, a potent inhibitor of FGFR1, FGFR2, FGFR3, and FGFR4 (FGFR1-4) kinases (Table 1).

**Table 1.** Biochemical and cellular inhibitory activity of JNJ-42756493

JNJ-42756493				
Kinases	Kd (nmol/L)	Kinases	IC <sub>50</sub> (nmol/L)	± SD
FGFR1	0.24	FGFR1	1.2	0.4
RET	0.94	FGFR2	2.5	0.9
FGFR3	1.1	FGFR3	3	0.5
FGFR4	1.4	FGFR4	5.7	0.8
FGFR2	2.2	VEGFR2	36.8	7.1
CSF1R	3.4	Kinases	BaF3 IC <sub>50</sub> (nmol/L)	± SEM
PDGFRA	3.4	FGFR1	22.1	0.81
FLT4	3.6	FGFR3	13.2	0.47
PDGFRB	4.6	FGFR4	25	0.3
KIT	5.3	VEGFR2	1160	30.7
VEGFR2	6.6	RET	205.2	25.7 <sup>a</sup>
TIE1	9	PDGFRA	156.2	51.2 <sup>a</sup>
FLT1	12	PDGFRB	304.1	119.6 <sup>a</sup>
EPHA1	13	KIT	>3,000	N/A
LCK	20	TIE1	>3,000	N/A
LYN	22	LCK	>3,000	N/A
ABL1	23	LYN	646.4	197.5 <sup>a</sup>
EPHB6	32	ABL1	>3,000	N/A
BLK	44	BLK	5,514.2	567.6 <sup>a</sup>
DDR1	45			
Cell line	Origin	FGFR alteration	IC <sub>50</sub> nmol/L	± SEM
KATO III	Gastric	FGFR2 (Amp)	0.1	0.01
SNU-16	Gastric	FGFR2 (Amp)	0.4	0.02
RT-112	Bladder	FGFR3 (translocation)	1.3	0.2
NCI-H1581	Large cell lung	FGFR1 (Amp)	2.6	0.2
A-204	Rhabdomyosarcoma	FGFR4 (Amp)	4.5	0.4
RT-4	Bladder	FGFR3 (translocation)	5.1	0.6
DMS-114	Small cell lung	FGFR1 (Amp)	7.0	1.2
A-427	Squamous lung	FGFR1 (Amp)	71.0	25.6
KMS-11	Multiple myeloma	FGFR3 (translocation)	102.4	53.6
MDA-MB-453	Breast	FGFR4 (Y367C)	129.2	30.4

<sup>a</sup>± SD.

JNJ-42756493 inhibited the tyrosine kinase activities of FGFR1-4 in time-resolved fluorescence assays with  $IC_{50}$  values of 1.2, 2.5, 3.0, and 5.7 nmol/L, respectively. The closely related VEGFR2 kinase was less potently inhibited (~30-fold less potent compared with FGFR1) by JNJ-42756493, with an  $IC_{50}$  value of 36.8 nmol/L.

The binding affinity of JNJ-42756493 was tested against a panel of 451 kinases (Supplementary Table S1) using the KINOMEScan platform (DiscoverX; ref. 19). The 20 kinases with the highest binding affinity are shown in Table 1. JNJ-42756493 bound FGFR1, 3, 4, and 2 with  $K_d$  values of 0.24, 1.1, 1.4, and 2.2 nmol/L, respectively. The  $K_d$  value for VEGFR2 was somewhat higher at 6.6 nmol/L.

The potent kinase binding and inhibitory activities of JNJ-42756493 observed on the isolated recombinant FGFR kinases were recapitulated in BaF3 cell lines engineered to express FGFR family members. JNJ-42756493 inhibited proliferation of FGFR1, 3, and 4 expressing cells with  $IC_{50}$  values of 22.1, 13.2, and 25 nmol/L, respectively (Table 1). The specificity of JNJ-42756493 activity in these cells was confirmed by the absence of effects on proliferation in the presence of IL3 ( $IC_{50} > 7,000$  nmol/L for all cell lines tested). In contrast, with the relatively potent activities against VEGFR2 in biochemical assays, JNJ-42756493 demonstrated substantially weaker activity against BaF3 cells expressing VEGFR2 ( $IC_{50} = 1,160$  nmol/L; Table 1). Similarly, JNJ-42756493 was at least 10 times more potent on BaF3 cells expressing FGFR kinases than other kinases with high-binding affinities (RET, PDGFRA, PDGFRB, KIT, TIE1, LCK, LYN, ABL1, and BLK). To confirm that selectivity of JNJ-42756493 for FGFRs versus VEGFR was compound dependent and not assay related, brigatinib (BMS-540215), a dual VEGFR/FGFR inhibitor, was tested in the same biochemical and BaF3 cellular kinase assays. In contrast to JNJ-42756493, brigatinib demonstrated higher potency against VEGFR2 compared with FGFRs (Supplementary Table S2), consistent with previous reports (27). Collectively, these results highlight the biochemical and functional selectivity of JNJ-42756493 for the FGFR family with limited off-target activity against VEGFR2 and other kinases.

### Cellular activity of JNJ-42756493 and inhibition of downstream signaling

As demonstrated in Fig. 1A, JNJ-42756493 effectively inhibited pFGFR1, pFGFR3, and pFGFR4 at 100 nmol/L in NCI-H1581, KMS-11, and MDA-MB-453 cells, respectively, and pFGFR2 at 30 nmol/L in SNU-16 cells. Inhibition of FGFR auto-phosphorylation was consistent with its antiproliferative  $IC_{50}$ s in these cell lines (2.6, 0.40, 102.4, and 129.2 nmol/L, for NCI-H1581, SNU-16, KMS-11, and MDA-MB-453, respectively; Table 1). The inhibitory activity of JNJ-42756493 on proliferation was confirmed in several additional cell lines with FGFR alterations from multiple cancer types (Table 1).

The inhibitory activity of JNJ-42756493 on signal transduction pathways downstream of FGFR was assessed in NCI-H1581, a lung cancer cell line with a focal *FGFR1* gene amplification (Fig. 1B). To activate downstream signaling, cells were stimulated with FGF2 ligand. In DMSO pretreated samples, robust FGFR pathway activation was detected within 5 minutes of ligand addition, as evidenced by higher levels of pFGFR and pFRS2 (FGFR adaptor protein), as well as increased phosphorylation of phospholipase C  $\gamma$  1 (pPLC $\gamma$ 1) and Extracellular Signal Receptor Regulated Kinase 1 and 2 (pERK1/2). Pretreatment with JNJ-42756493 for 1 hour prior to addition of the FGF2 ligand, led to inhibition of downstream signaling, evidenced by decreased levels of pFGFR, pFRS2, pPLC $\gamma$ 1, and pERK1/2. Taken together, these data demonstrate cellular pan-FGFR kinase inhibition by JNJ-42756493 leading to modulation of FGFR downstream signaling.

### Potent antiproliferative activity of JNJ-42756493 on FGFR-altered cancer cell lines

The antiproliferative selectivity of a close analogue of JNJ-42756493, JNJ-42541707 (Supplementary Fig. S1A) was tested against a large panel of human cancer cell lines of diverse tissue origin. Sensitivity ( $IC_{50} < 1$   $\mu$ mol/L) was observed in a subset of the tumor cell lines and largely correlated with overexpression of FGFR family members (Supplementary Fig. S1B). A similar analysis using a slightly different panel of cancer cell lines was

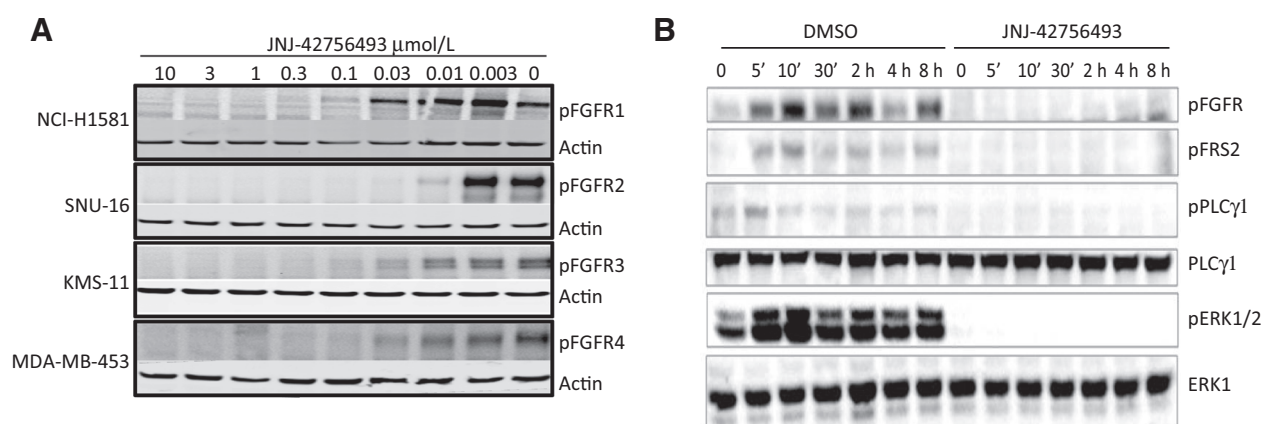


**Figure 1.**

JNJ-42756493 inhibits FGFR auto-phosphorylation in cancer cell lines with activated FGFR1-4 and FGFR-dependent signaling in NCI-H1581 cells. **A**, Western blots of phospho-FGFR (pFGFR) and protein loading control actin in human cancer cell lines containing FGFR1-4 alterations following treatment with multiple JNJ-42756493 concentrations. **B**, Western blots of several phospho-proteins in FGFR signaling pathway and loading control proteins PLC $\gamma$ 1 and ERK1 in NCI-H1581 cells pretreated with DMSO or JNJ-42756493, then stimulated for indicated length of time with FGF2.

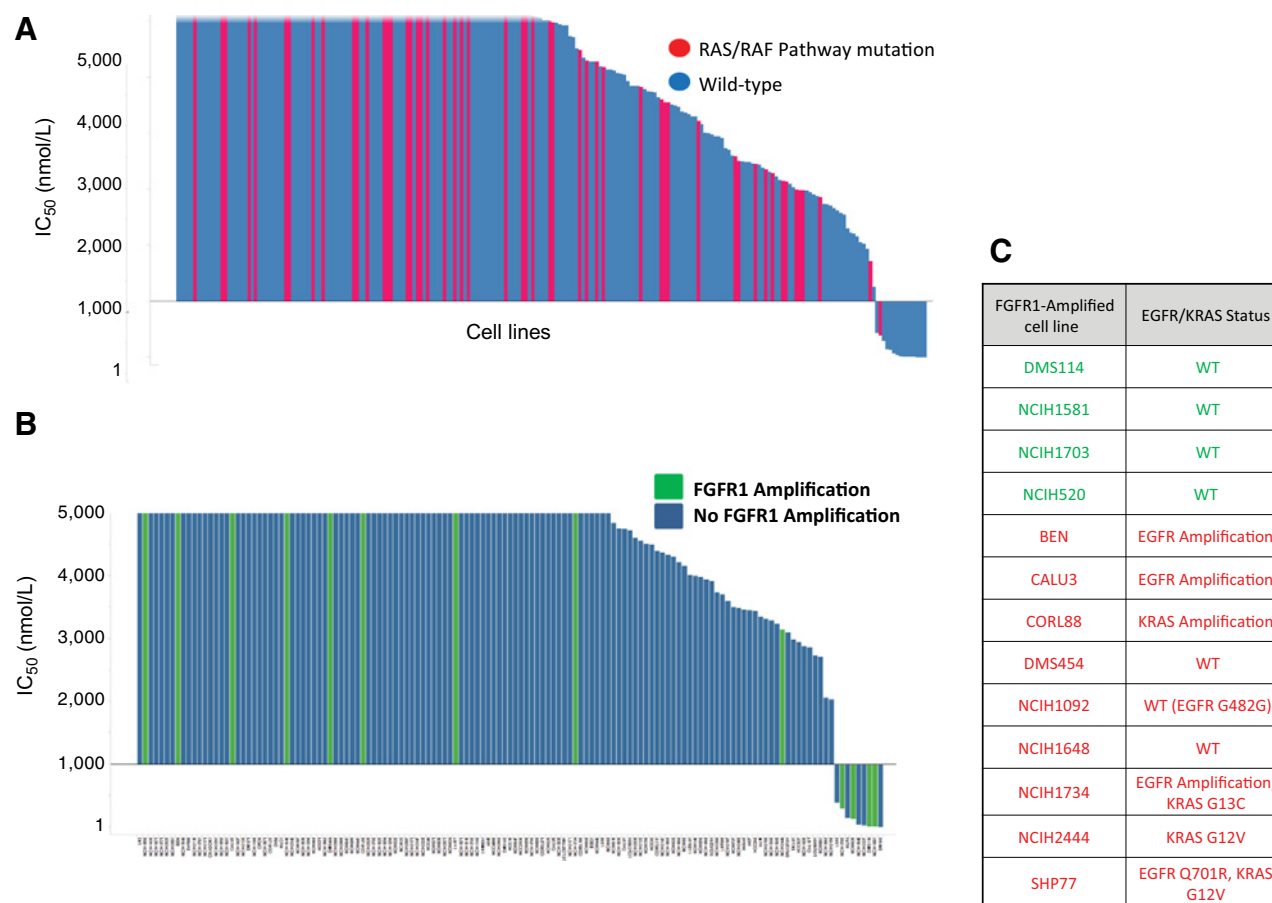


**Figure 2.**

JNJ-42756493 antiproliferative activity against human cancer cell lines. JNJ-42756493 growth inhibition ( $IC_{50}$ ) of cancer cell lines (A) from multiple origin ( $n = 236$ ) and color coded based on RAS/RAF status (B) from lung cancer origin ( $n = 136$ ) and color coded based on FGFR1 focal DNA amplification. C, Subset of lung cancer cell lines with FGFR1 amplification color coded based on JNJ-42756493 sensitivity (green:  $IC_{50} < 1,000$  nmol/L, red:  $IC_{50} > 1,000$  nmol/L) and with their corresponding RAS/EGFR status.

performed with JNJ-42756493. Interestingly, in addition to a correlation of sensitivity with FGFR overexpression, a large fraction of insensitive tumor cell lines harbored mutations in RAS or RAF, indicating that alterations downstream of FGFR can overcome the effects of FGFR inhibition (Fig. 2A; underlying data on Supplementary Table S3). The majority of cell lines tested were not sensitive to the inhibitor ( $IC_{50} > 5$   $\mu\text{mol/L}$ ), highlighting its selectivity and confirming a lack of appreciable non-FGFR off-target activity.

To further understand the FGFR antiproliferative relationship, we extended testing to a broad panel of lung cancer cell lines. JNJ-42756493 activity in a panel of 145 lung cancer cell lines was associated with FGFR1 amplification status (Fig. 2B). However, not all lung cancer cell lines with FGFR1 amplification were sensitive to JNJ-42756493. Most of the insensitive tumor cell lines were found to co-harbor other known oncogenic mutations within the EGFR/KRAS pathway (Fig. 2C), indicating that these pathways may be more dominant oncogenic drivers in this context. The molecular determinants of cell lines sensitive to JNJ-42756493 between 1 and 5  $\mu\text{mol/L}$  is unknown, but could be due to alternative FGFR-activating mechanisms, such as chromosomal translocations, or FGFR-unrelated activities of JNJ-

42756493. Taken together, our results highlight the functional selectivity of JNJ-42756493 for FGFR-altered pathway without concomitant MAPK pathway alterations.

#### Intracellular lysosomal localization of JNJ-42756493 results in sustained pathway inhibition

Imaging of cells treated with JNJ-42756493, which is intrinsically fluorescent, revealed an intracellular staining pattern similar to that of the lysosomal marker LysoTracker, consistent with lysosomal accumulation (Fig. 3A). Addition of bafilomycin, a specific inhibitor of the vacuolar-type  $H^+$ -ATPase that increases lysosomal pH, reduced lysosomal accumulation of LysoTracker Red and JNJ-42756493 (Fig. 3B), but had little or no effect on the subcellular distribution or accumulation of JNJ-42883919, another fluorescent FGFR inhibitor from the same chemical series as JNJ-42756493 (Fig. 3C). Time course analysis demonstrated rapid uptake and intracellular accumulation of JNJ-42756493 that was prevented by pretreatment of the cells with bafilomycin (Fig. 3E).

Because JNJ-42756493 appears to accumulate to high concentrations in lysosomes, we speculated that this property of the compound might contribute to persistent FGFR kinase

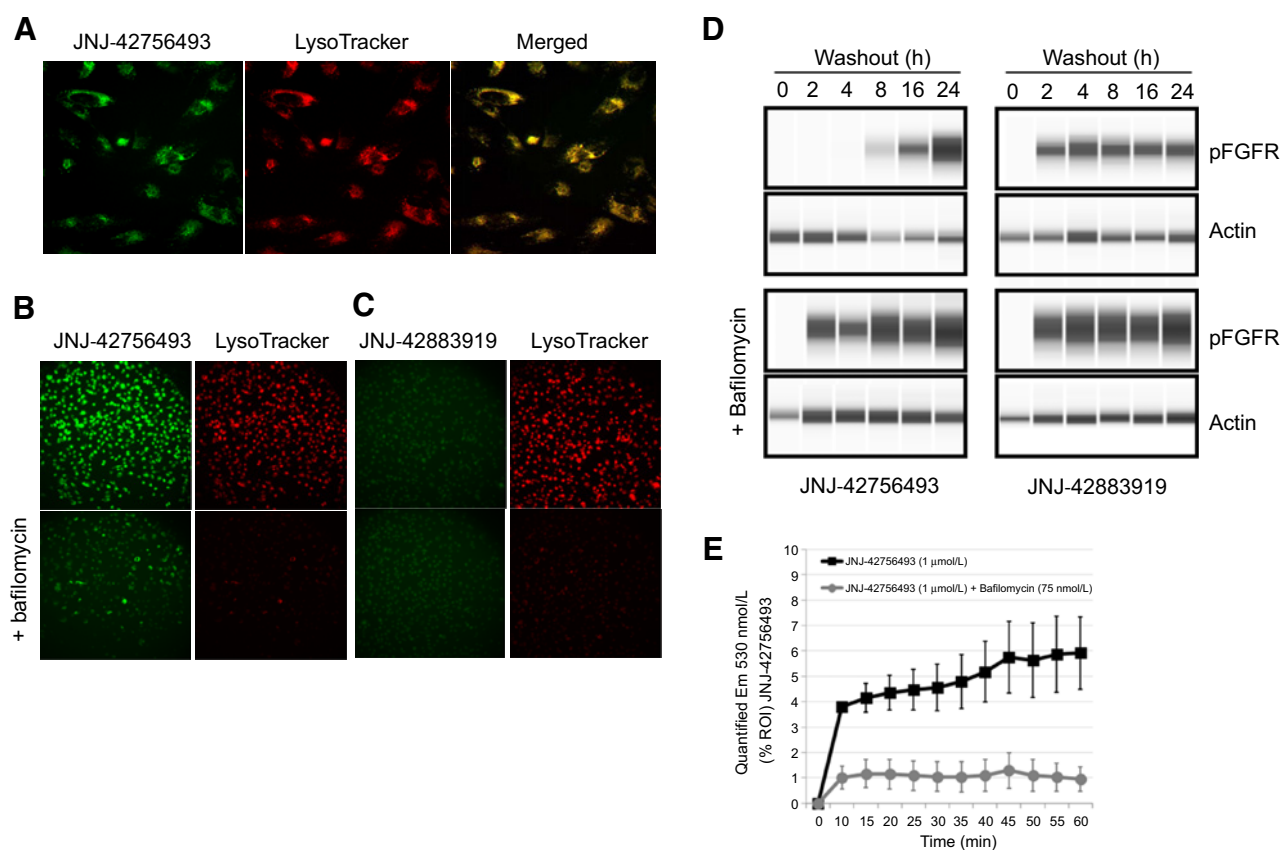


**Figure 3.**

Lysosomal accumulation of JNJ-42756493 and sustained inhibition of FGFR following compound washout. GAMG cells showing (A) intrinsic fluorescence of JNJ-42756493 (green), fluorescence of a lysosome staining probe (LysoTracker, red), and merging of the 2 images (merged, yellow). B, Reduced lysosomal fluorescence intensity of JNJ-42756493 and LysoTracker in the presence of bafilomycin (C) absence of changes in JNJ-42883919 fluorescence intensity compared with LysoTracker in the presence of bafilomycin. D, Sustained inhibition of pFGFR following washout of KATO III cells pretreated with JNJ-42756493 compared with cells pretreated with JNJ-42756493 and bafilomycin or pretreated with JNJ-42883919 with and without bafilomycin. Western blot analysis of actin as loading control. E, Fluorescence signal (530 nm) in GAMG cells treated with JNJ-42756493 in the presence or absence of bafilomycin compared with T = 0 in region of interest (% ROI).

inhibition in cells. KATO III cells were treated with JNJ-42756493 or the non-lysosomotropic analogue, JNJ-42883919, for 1 hour, and FGFR2 inhibition (pFGFR) assessed following compound washout. The pFGFR signal was completely inhibited by JNJ-42756493 up to 4 hours, returning to basal levels 24 hours after washout (Fig. 3D). In stark contrast, pFGFR levels in cells treated with JNJ-42883919 returned to basal levels within 2 hours. Pretreatment of the cells with bafilomycin reversed sustained target inhibition by JNJ-42756493, as evidenced by detection of pFGFR at basal levels 2 hours after washout (Fig. 3D). Bafilomycin treatment did not alter the duration of pFGFR inhibition by the non-lysosomotropic analogue JNJ-42883919. These data highlight the unique lysosomal accumulating properties of JNJ-42756493 that contribute to prolonged FGFR inhibition, possibly as a consequence of sustained release of the inhibitor over time.

#### JNJ-42756493 antitumor activity is associated with inhibition of FGFR downstream signaling

We next assessed *in vivo* efficacy of JNJ-42756493 on tumors with FGFR alterations. Animals bearing xenograft tumors derived

from SNU-16 human gastric cancer cells harboring *FGFR2* amplifications were treated orally with vehicle or JNJ-42756493 at various doses. Upon administration, JNJ-42756493 reached maximal plasma concentration at 0.5 hour and returned to undetectable levels [lower limit of quantification (LLOQ) = 0.4 ng/mL] by 7 hours for the 3 mg/kg dose, and 16 hours for the 10 and 30 mg/kg doses. No significant inhibition of downstream FGFR signaling was observed in tumor lysates from mice treated with 3 mg/kg JNJ-42756493 (Fig. 4A). However, FGFR signaling was significantly inhibited, starting from 1 hour after administration until 7 and 16 hours, in mice treated with 10 (Fig. 4B) and 30 mg/kg (Fig. 4C) of JNJ-42756493, respectively. Significant inhibitor-dependent modulation of pERK was not consistently observed in this tumor model. The reasons are unknown, but could be due to technical reasons, such as the presence of mouse stromal cells with reactivity to the pERK antibody. Nevertheless, JNJ-42756493 resulted in dose-dependent tumor growth inhibition (TGI) in SNU-16 tumor-bearing mice. Treatment with 10 and 30 mg/kg JNJ-42756493 daily for 21 days resulted in TGI of 37.8% and 59.4%, respectively (Fig. 4D). Similar antitumoral effects were observed in several other tumor models (MDA-MB-453, SNU-16,

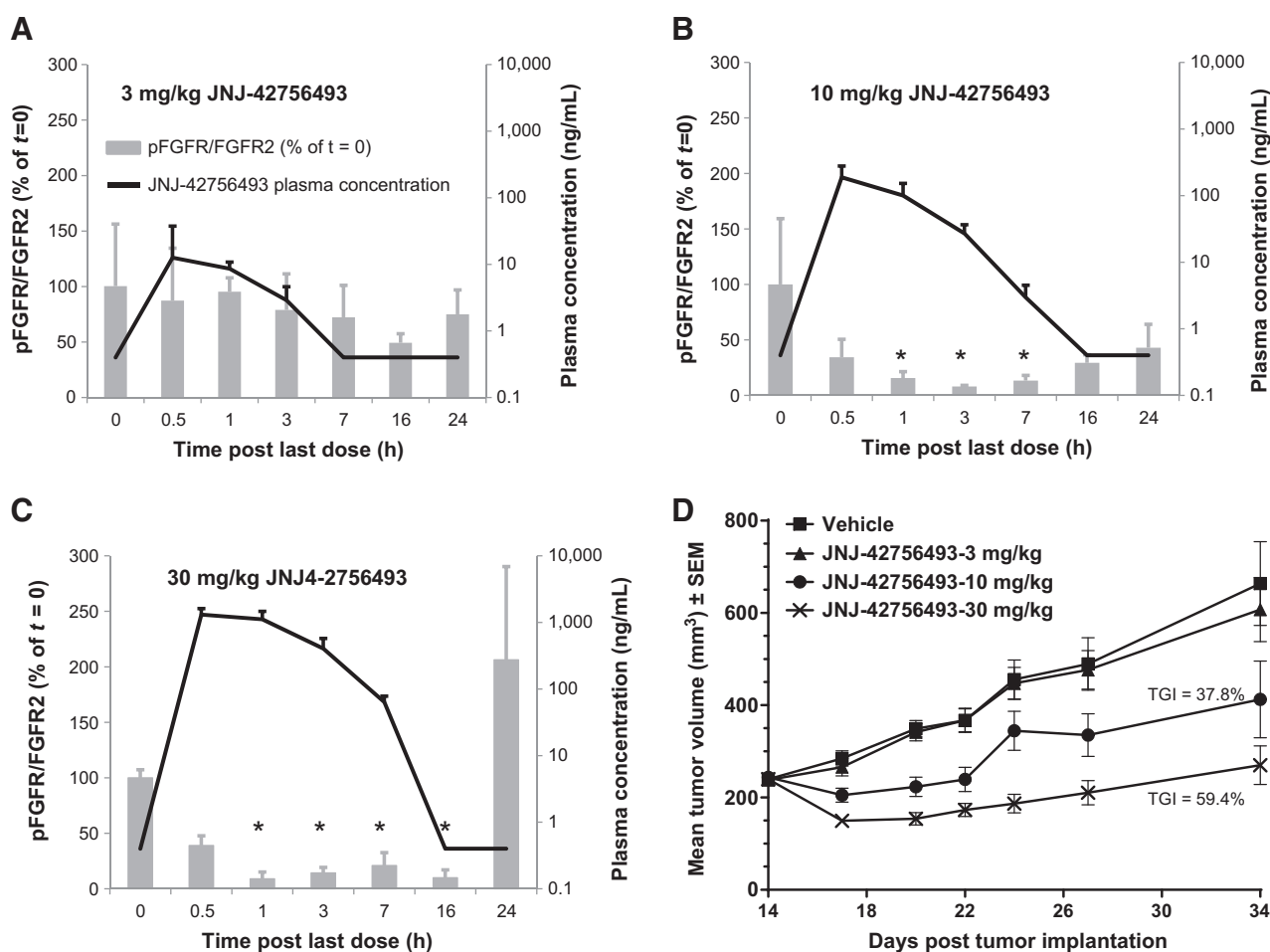


**Figure 4.**

Relationship between *in vivo* JNJ-42756493 plasma concentration, inhibition of pFGFR2, and efficacy in SNU-16 human gastric xenograft mouse model. Animals were treated with JNJ-42756493 at (A) 3 mg/kg, (B) 10 mg/kg or (C) 30 mg/kg QD. Tumor and blood from 3 animals per group were harvested after single first dose at indicated time points for analysis of pFGFR/FGFR2 by Western blot analysis [(left axis (gray bars), significant ( $P < 0.001$ ) difference compared to  $T=0$  is marked with asterisks) and plasma compound concentration (right axis, LLOQ = 0.4 mg/mL, black line), respectively. D, Efficacy of JNJ-42756493 was evaluated at 0 (vehicle), 3, 10, and 30 mg/kg QD treatment for 21 days. Significant percent tumor growth inhibition (%TGI) of compound compared to vehicle treated animals is indicated at efficacious doses.

NCI-H1581, A-204, HuH-7, NCI-H716, and RT112) with a variety of different *FGFR* alterations (Supplementary Table S4).

In addition to gene amplification or overexpression, *FGFRs* can be constitutively activated by chromosomal rearrangement (7, 28). However, *FGFR* gene translocations are rarely present in existing xenograft models derived from cancer cell lines. To examine the dependency of tumors with *FGFR* translocations to JNJ-42756493, we surveyed a collection of patient-derived explant xenograft (PDX) models for *FGFR* genetic alterations and identified LUX001 [human non-small cell lung cancer (NSCLC)] that contains a translocation resulting in expression of a *FGFR3-TACC3* fusion protein. LUX001-tumor (~400 mm<sup>3</sup>) bearing mice were treated with JNJ-42756493 for 21 days at 12.5 mg/kg twice a day (BID). Blood and tumors were collected before ( $t = 0$ ) and after first dosing with JNJ-42756493 for determination of concentration of the inhibitor in plasma and pERK inhibition in tumors (Fig. 5A). Similar to our observations in *FGFR*-amplified models (Fig. 4), JNJ-42756493 treatment

resulted in maximal plasma concentration at approximately 1 hour posttreatment, which was accompanied by suppression of constitutive pERK signaling observed in this model. In this model, reduced plasma concentrations of the inhibitor were associated with decreased pERK suppression. Importantly, JNJ-42756493 resulted in pronounced antitumor activity (TGI = 100%) in LUX001 tumor-bearing mice treated, suggesting that tumors harboring *FGFR* translocations are highly dependent upon this genetic activation event (Fig. 5B). These results demonstrated that the *FGFR* selective inhibitor JNJ-42756493 has potent *in vivo* activity on tumors with a variety of different *FGFR* genetic alterations.

## Discussion

Targeted therapies against key activating genetic mutations have become standard of care for a variety of cancer subtypes. These developments have encouraged the field to mount new



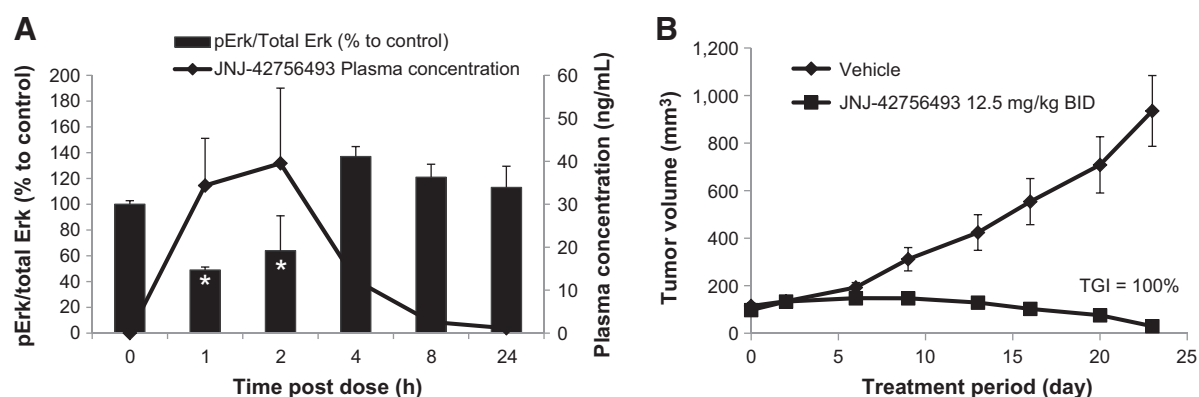


**Figure 5.**

Relationship between *in vivo* JNJ-42756493 plasma concentration, inhibition of pERK and efficacy in LUX001 PDX with FGFR3-TACC3 fusion mouse model. Animals were treated with vehicle or JNJ-42756493 at 12.5 mg/kg BID. **A**, At indicated time (0, 1, 2, 4, 8, and 24 hours) post-first dosing, blood and tumors from 3 animals per group were harvested for plasma compound concentration (right axis) and level pERK/Total-Erk by quantified Western blot analysis (left axis, significant ( $P < 0.001$ ) difference compared to T = 0 is marked with asterisks), respectively. **B**, Efficacy of JNJ-42756493 was evaluated and percent tumor growth inhibition (%TGI) of compound compared with vehicle treated animals is indicated.

drug-discovery efforts against emerging pathways such as FGFR, which has been observed to be activated at significant frequency in a variety of cancers (1). However, it is not clear whether the observed mutations are bystander events or bona fide genetic drivers, particularly in tumor types, such as lung cancer with high mutational burden. Furthermore, confirmation of the oncogenic dependency on specific kinases using small molecule inhibitors that are not selective for the target of interest is complicated by off-target activities that can inhibit other anti-proliferative pathways and/or can be associated with toxicities limiting therapeutic utility. Thus, highly selective inhibitors, such as JNJ-42756493, can be useful tools for determining the dependency of tumors on oncogenic driver pathways, such as FGFR, and may reduce the risk of off-target adverse events. Clinical data obtained with JNJ-42756493 so far are consistent with the hypothesis supporting absence of appreciable VEGFR2 inhibitory activity (29).

Our data highlight the functional selectivity of JNJ-42756493 for the FGFR family in a variety of model systems. First, unlike first-generation mixed FGFR/VEGFR inhibitors, such as brivanib, which are more potent against VEGFR than FGFR (30), JNJ-42756493 demonstrated greater than 50-fold selectivity over VEGFR2 in cellular assays. Second, broad *in vitro* antiproliferative profiling of tumor cell lines with JNJ-42756493 revealed that sensitivity was associated with FGFR overexpression or amplification, whereas insensitivity was associated with the activation of other oncogenic pathways. Interestingly, the majority of tumor cell lines with FGFR aberrations that were resistant to JNJ-42756493 harbored additional mutations in RAS or RAF family members, indicating that mutations downstream of the receptor tyrosine kinase can bypass dependency on the receptor. These observations are consistent with what has been reported for EGFR and downstream KRAS mutations (31, 32) and have clinical implications for the use of anti-EGFR agents, such as cetuximab, which are not indicated in colorectal cancer patients with KRAS alterations (33). Our data have similar clinical implications suggesting that patient co-harboring FGFR mutations and downstream RAS or RAF mutations are not likely to be sensitive to pathway inhibition by JNJ-42756493.

A consequence of FGFR activation is the phosphorylation of downstream signal transducers, such as FRS2 and ERK2 (34). We observed a strong correlation between levels of JNJ-42756493 and the suppression of FGFR auto-phosphorylation and downstream signaling events *in vitro*. Similarly, we observed sustained inhibition of pFGFR and pERK following administration of JNJ-42756493 in xenograft and PDX models, respectively. The reasons for the absence of pERK modulation in the xenograft model described are unclear, but pERK modulation in a patient-derived xenograft with an activating *FGFR3-TACC3* translocation resulted in a robust antitumor activity. Similarly, patients harboring FGFR2 or FGFR3 translocations have also shown response to JNJ-42756493 treatment (29). It is not clear whether antitumor efficacy is driven by maximum concentration ( $C_{max}$ ), total area under the curve (AUC), or prolonged trough concentration ( $C_{trough}$ ) levels. The transient decrease in pERK after JNJ-42756493 administration suggests that sustained exposure over a threshold rather than  $C_{max}$  exposure is more closely associated with efficacy. In this regard, it is interesting to note that JNJ-42756493 accumulates in lysosomes, which can potentially serve as a depot for sustained release of the compound and result in more prolonged pathway inhibition.

There is increasing interest in targeting FGFR for cancer therapy due to its activation by point mutation, amplification, or chromosomal rearrangement (1) in a variety of tumors. Activating FGFR gene rearrangements were first identified in a search for novel oncogenes in osteosarcoma. *FGFR2-FRAG1* was characterized as a potent oncogene consisting of FGFR2 with a C-terminal fusion of the FRAG1 dimerization sequence that promoted constitutive activation of the chimeric protein (35). This observation was recently extended clinically with the identification of multiple C-terminal fusion partners across most of the FGFR family members (36, 37) broadening the range of genetic alterations from known point mutations and gene amplification events. However, it is not clear if all these alterations confer equivalent dependency to tumor cells with a given FGFR alteration. *In vitro*, the impact of JNJ-42756493 on cell proliferation was evident in cancer cell lines of diverse tissue origin carrying amplifications in FGFR family members. Although the cell line panel tested in this study did not

contain tumor cells with FGFR translocations, we have since shown potent antiproliferative effects in BaF3-FGFR3-TACC3-engineered cells (J.D. Karkera; personal communication), suggesting that this is also a dominant oncogenic event. However, *in vivo*, our results suggest that JNJ-42756493 is more potent in models with FGFR translocations compared with those with amplifications, implying that there is a hierarchy of dependency amongst the different FGFR genetic alterations. Nonetheless, these results support the clinical evaluation of JNJ-42756493 (29) in malignancies and other disorders associated with constitutively activated FGFR signaling.

### Disclosure of Potential Conflicts of Interest

T.P.S. Perera has ownership interest (including patents) in JNJ. G. Saxty is an inventor on the patent but does not financially benefit. M. Page is a consultant/advisory board member for Astex Pharma. D.R. Newell is a consultant for Astex Pharma, reports receiving a commercial research grant from Astex Pharma, and is a consultant/advisory board for Astex Pharma. No potential conflicts of interest were disclosed by the other authors.

### Authors' Contributions

**Conception and design:** T.P.S. Perera, J. Vialard, P. King, E. Freyne, M. Squires, G. Saxty, R. Gilissen, C.W. Murray, N.T. Thompson, D.R. Newell, L. Xie, P. Angibaud, S. Laquerre, M.V. Lorenzi

**Development of methodology:** T.P.S. Perera, L. Mevellec, J. Vialard, D.D. Lange, P. King, M. Squires, D.R. Newell, N. Cheng, P. Angibaud, S. Laquerre, S.J. Platero, E. Jovcheva, E. Freyne, G. Saxty

**Acquisition of data (provided animals, acquired and managed patients, provided facilities, etc.):** L. Mevellec, D.D. Lange, T. Verhulst, C. Paulussen, K.V.D. Ven, P. King, G. Ward, N. Cheng, J.D. Karkera

**Analysis and interpretation of data (e.g., statistical analysis, biostatistics, computational analysis):** T.P.S. Perera, J. Vialard, T. Verhulst, P. King, E. Freyne, D.C. Rees, M. Squires, S.J. Platero, G. Saxty, R. Gilissen, L. Xie, C. Moy, P. Angibaud, S. Laquerre

**Writing, review, and/or revision of the manuscript:** T.P.S. Perera, L. Mevellec, J. Vialard, D.D. Lange, T. Verhulst, P. King, R. Gilissen, C.W. Murray, L. Xie, J.D. Karkera, P. Angibaud, S. Laquerre, M.V. Lorenzi

**Administrative, technical, or material support (i.e., reporting or organizing data, constructing databases):** J. Vialard, T. Verhulst, C. Moy

**Study supervision:** T.P.S. Perera, J. Vialard, M. Page, N.T. Thompson, L. Xie, J. Yang, S. Laquerre, E. Freyne, G. Saxty

The costs of publication of this article were defrayed in part by the payment of page charges. This article must therefore be hereby marked *advertisement* in accordance with 18 U.S.C. Section 1734 solely to indicate this fact.

Received November 21, 2016; revised December 28, 2016; accepted March 15, 2017; published OnlineFirst March 24, 2017.

### References

- Hallinan N, Finn S, Cuffe S, Rafee S, O'Byrne K, Gately K. Targeting the fibroblast growth factor receptor family in cancer. *Cancer Treat Rev* 2016;46:51–62.
- Wesche J, Haglund K, Haugsten EM. Fibroblast growth factors and their receptors in cancer. *Biochem J* 2011;437:199–213.
- Touat M, Ileana E, Postel-Vinay S, Andre F, Soria JC. Targeting FGFR Signaling in Cancer. *Clin Cancer Res* 2015;21:2684–94.
- Itoh N, Ornitz DM. Functional evolutionary history of the mouse Fgf gene family. *Dev Dyn* 2008;237:18–27.
- Dienstmann R, Rodon J, Prat A, Perez-Garcia J, Adamo B, Felip E, et al. Genomic aberrations in the FGFR pathway: opportunities for targeted therapies in solid tumors. *Ann Oncol* 2014;25:552–63.
- Lim SM, Kim HR, Shim HS, Soo RA, Cho BC. Role of FGF receptors as an emerging therapeutic target in lung squamous cell carcinoma. *Future Oncol* 2013;9:377–86.
- Wu YM, Su F, Kalyana-Sundaram S, Khazanov N, Ateeq B, Cao X, et al. Identification of targetable FGFR gene fusions in diverse cancers. *Cancer Discov* 2013;3:636–47.
- Schildhaus HU, Nogova L, Wolf J, Buettner R. FGFR1 amplifications in squamous cell carcinomas of the lung: diagnostic and therapeutic implications. *Transl Lung Cancer Res* 2013;2:92–100.
- Williams SV, Hurst CD, Knowles MA. Oncogenic FGFR3 gene fusions in bladder cancer. *Hum Mol Genet* 2013;22:795–803.
- Katoh M, Nakagama H. FGF receptors: cancer biology and therapeutics. *Med Res Rev* 2014;34:280–300.
- Penault-Llorca F, Bertucci F, Adelaide J, Parc P, Coulier F, Jacquemier J, et al. Expression of FGF and FGF receptor genes in human breast cancer. *Int J Cancer* 1995;61:170–6.
- Matsumoto K, Arai T, Hamaguchi T, Shimada Y, Kato K, Oda I, et al. FGFR2 gene amplification and clinicopathological features in gastric cancer. *Br J Cancer* 2012;106:727–32.
- Tsujimoto H, Sugihara H, Hagiwara A, Hattori T. Amplification of growth factor receptor genes and DNA ploidy pattern in the progression of gastric cancer. *Virchows Arch* 1997;431:383–9.
- Marian C, Ochs-Balcom HM, Nie J, Kallakury BV, Ambrosone CB, Trevisan M, et al. FGFR2 intronic SNPs and breast cancer risk: associations with tumor characteristics and interactions with exogenous exposures and other known breast cancer risk factors. *Int J Cancer* 2011;129:702–12.
- Spinola M, Leoni V, Pignatiello C, Conti B, Ravagnani F, Pastorino U, et al. Functional FGFR4 Gly388Arg polymorphism predicts prognosis in lung adenocarcinoma patients. *J Clin Oncol* 2005;23:7307–11.
- Dieci MV, Arnedos M, Andre F, Soria JC. Fibroblast growth factor receptor inhibitors as a cancer treatment: from a biologic rationale to medical perspectives. *Cancer Discov* 2013;3:264–79.
- Tanner Y, Grose RP. Dysregulated FGF signalling in neoplastic disorders. *Semin Cell Dev Biol* 2016;53:126–35.
- Katoh M. FGFR inhibitors: Effects on cancer cells, tumor microenvironment and whole-body homeostasis (Review). *Int J Mol Med* 2016;38:3–15.
- Fabian MA, Biggs WH3rd, Treiber DK, Atteridge CE, Azimioara MD, Benedetti MG, et al. A small molecule-kinase interaction map for clinical kinase inhibitors. *Nat Biotechnol* 2005;23:329–36.
- Daley GQ, Baltimore D. Transformation of an interleukin 3-dependent hematopoietic cell line by the chronic myelogenous leukemia-specific P210bcr/abl protein. *Proc Natl Acad Sci U S A* 1988;85:9312–6.
- Squires M, Ward G, Saxty G, Berdini V, Cleasby A, King P, et al. Potent, selective inhibitors of fibroblast growth factor receptor define fibroblast growth factor dependence in preclinical cancer models. *Mol Cancer Ther* 2011;10:1542–52.
- atcc.org [Internet]. American Type Culture Collection; c2016 [cited 2016 Aug 26]. Available from: <http://www.atcc.org/>.
- dsmz.de [Internet]. German Collection of Microorganisms and Cell Cultures, Germany; c1998–2015 [cited 2016 Aug 26]. Available from: <http://www.dsmz.de/>.
- cellbank.nibiohn.go.jp [Internet]. Japanese Collection of Research Bioresources, Japan; c2005–2015 [cited 2016 Aug 26]. Available from: <http://cellbank.nibiohn.go.jp/>.
- United Kingdom Co-ordinating Committee on Cancer Research (UKCCCR) Guidelines for the welfare of animals in experimental neoplasia (Second Edition). *Br J Cancer* 1998;77:1–10.
- Bissery MC, Chabot GG. History and new development of screening and evaluation methods of anticancer drugs used *in vivo* and *in vitro*. *Bull Cancer* 1991;78:587–602.
- Diaz-Padilla I, Siu LL. Brivanib alaninate for cancer. *Expert Opin Investigat Drugs* 2011;20:577–86.
- Costa R, Carneiro BA, Taxter T, Tavora FA, Kalyan A, Pai SA, et al. FGFR3-TACC3 fusion in solid tumors: mini review. *Oncotarget* 2016;7:55924–38.
- Tabernero J, Bahleda R, Dienstmann R, Infante JR, Mita A, Italiano A, et al. Phase I dose-escalation study of JNJ-42756493, an oral pan-fibroblast growth factor receptor inhibitor, in patients with advanced solid tumors. *J Clin Oncol* 2015;33:3401–8.

30. Cai ZW, Zhang Y, Borzilleri RM, Qian L, Barbosa S, Wei D, et al. Discovery of brivanib alaninate ((S)-((R)-1-(4-(4-fluoro-2-methyl-1H-indol-5-yloxy)-5-methylpyrrolo[2,1-f][1,2,4] triazin-6-yloxy)propan-2-yl)2-aminopropanoate), a novel prodrug of dual vascular endothelial growth factor receptor-2 and fibroblast growth factor receptor-1 kinase inhibitor (BMS-540215). *J Med Chem* 2008;51:1976–80.
31. Young A, Lou D, McCormick F. Oncogenic and wild-type Ras play divergent roles in the regulation of mitogen-activated protein kinase signaling. *Cancer Discov* 2013;3:112–23.
32. Benvenuti S, Sartore-Bianchi A, Di Nicolantonio F, Zanon C, Moroni M, Veronese S, et al. Oncogenic activation of the RAS/RAF signaling pathway impairs the response of metastatic colorectal cancers to anti-epidermal growth factor receptor antibody therapies. *Cancer Res* 2007;67:2643–8.
33. Lievre A, Bachet JB, Boige V, Cayre A, Le Corre D, Buc E, et al. KRAS mutations as an independent prognostic factor in patients with advanced colorectal cancer treated with cetuximab. *J Clin Oncol* 2008; 26:374–9.
34. Kouhara H, Hadari YR, Spivak-Kroizman T, Schilling J, Bar-Sagi D, Lax I, et al. A lipid-anchored Grb2-binding protein that links FGF-receptor activation to the Ras/MAPK signaling pathway. *Cell* 1997;89:693–702.
35. Lorenzi MV, Horii Y, Yamanaka R, Sakaguchi K, Miki T. FRAG1, a gene that potentially activates fibroblast growth factor receptor by C-terminal fusion through chromosomal rearrangement. *Proc Natl Acad Sci U S A* 1996; 93:8956–61.
36. Gallo LH, Nelson KN, Meyer AN, Donoghue DJ. Functions of Fibroblast Growth Factor Receptors in cancer defined by novel translocations and mutations. *Cytokine Growth Factor Rev* 2015;26:425–49.
37. Parker BC, Engels M, Annala M, Zhang W. Emergence of FGFR family gene fusions as therapeutic targets in a wide spectrum of solid tumours. *J Pathol* 2014;232:4–15.